

# Influence of soil structures on corrosion performance of floating-DC transit systems

C. Charalambous and I. Cotton

**Abstract:** The production of stray currents by DC-transit systems leads to the corrosion of nearby buried metallic structures, such as pipelines and cable sheaths. The paper details the corrosion performance of a DC transit system with a floating return rail, for a number of different soil-resistivity structures: uniform, horizontal and vertical-layer models. This builds on previous work carried out in homogenous soils. It is shown that a variation in soil type along the route of a transit system can lead to high local leakage-current densities on buried metallic structures, increasing their vulnerability to corrosion damage.

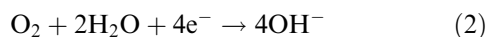
## 1 Introduction

Current leakage from DC-railway systems is an inevitable consequence of the use of the running rails as both a mechanical support/guideway and the return circuit for the traction supply current. Since the rails have a finite longitudinal, or series, resistance (around 40–80 mΩ/km) and a poor insulation from earth (typically from 2–100 Ω/km), a proportion of the traction current returning along them will leak to earth and flow along one of a number of parallel paths (either directly through the soil or through buried metallic conductors) before returning onto the rail and the negative terminal of the DC rectifier.

Given that current flow in a metallic conductor is electronic, while that through electrolytes such as the earth, concrete etc. is ionic, it follows that there must be an electron-to-ion transfer as current leaves the rails to earth. Where current leaves the rail to earth and an anode is produced, there will therefore be an oxidation, or electron-producing, reaction:



This reaction is visible after time as corrosion damage. For current to return onto the rail, there must be a reduction or electron-consuming reaction such as that normally observed on a cathodically protected system. In an oxygenated environment this will typically be as follows:



Note that the iron-reduction reaction is not thermodynamically preferred and that iron does not plate back onto the rail.

Corrosion of metallic objects will therefore occur at each point where current transfers from a metallic conductor, such as a reinforcement bar in concrete, to the electrolyte (i.e. the concrete) [1]. Hence stray-current leakage can cause corrosion damage to both the rails and any other surrounding metallic elements. In a few extreme cases,

severe structural damage has occurred as a result of stray-current leakage. There is therefore a stray-current-control requirement to minimise the impact of the stray current on the rail system, supporting infrastructure and third-party infrastructure.

This paper focuses on the impact of soil structures on the level of corrosion that will be observed on buried structures in the proximity of the DC transit system. The importance of this work is due to the major contribution of the soil resistivity in determining the path of any stray current that has already leaked from the traction system. In homogenous systems, high soil resistivities mean that third-party buried structures are generally less vulnerable to corrosion damage, while in low soil resistivities the converse is true [2].

Nonhomogenous soils have not typically been considered in stray-current analysis but are important, particularly when dealing with vertically layered soils. A sudden change in soil resistivity along the path of a transit system can, as will be shown, increase local current densities leading to higher risks of corrosion.

All of the case studies presented involve the simulation of a DC transit system with a floating return rail within the MALZ module of CDEGS software [3]. To analyse the flow of DC currents within a system in nonhomogenous soil, MALZ uses circuit theory and the method of images for multilayer soil following the technique developed by Oslon and Stankeeva [4]. Static models (i.e. where the train is at a fixed point in time) are used and these demonstrate the principles of the problem discussed.

## 2 Model system

### 2.1 Traction system and third-party structures

The essential elements of a transit system are the rails, the rail-to-earth insulation, the power supply and the vehicles. The design and placement of these elements of the transit system dictates the stray-current performance in terms of the total stray current leaving the rails.

The simulation model is based on a 1 km section of track used to illustrate the rail-to-earth voltage profile when a train draws current from a substation [5]. This 1 km section is representative of a symmetrical 2 km section of track with a single train at the centre and a substation at each end. The

train, placed at one end, is drawing the 1000 A that has been produced by a substation at the far end of the track.

For every 1 mΩ/km of track resistance, there will be a resulting voltage drop of 1 V/km along the rail. Take a case where the resistance of a single rail is 40 mΩ/km (20 mΩ/km for the track). For 1000 A current, the resulting voltage difference between the two ends of the track will be 20 V. In a floating system where the running rails (and hence the DC negative bus) are allowed to float with respect to earth, the voltage will appear on the rails as 10 V to remote earth near the train and -10 V to remote earth near the substation. Floating running rails are generally regarded as the best option if the stray current is to be minimised and are therefore the subject of this paper [5–7].

The voltages present on the rail cause current to leak into the earth where the voltage is positive and be collected from the earth where the voltage is negative. By determining the path of the stray current and how it flows onto/off buried structures, Faraday’s electrolytic formula [8] can be used to estimate the resultant corrosion damage.

As well as the running rails, the model system includes a stray-current-control mat and a buried pipe. The stray-current-control-mat, physically the reinforced concrete trackbed the running rail is mounted on, is intended to capture a large proportion of the stray current released by the running rail [5]. This should protect any third-party buried infrastructure that exists in the system, in this case the pipe. The details of the three elements modelled in the system are given in Table 1.

In cross-section, the ideal form of model to be employed is as shown in Fig. 1. The case where stray current is leaving the rails is illustrated. The stray current has three possible paths once it has left the rail: the trackbed, the buried service or the earth itself. Of particular note in the model is

**Table 1: Data employed in SESCAD conductors model**

Rail	Series resistance	0.04 Ω/km
	Resistance to earth	320 Ω/km
	Radius	0.048 m
	Number of conductors	1
	Buried at depth	0.05 m
Metallic mat	Series resistance	0.08 Ω/km
	Coating parameters	180 Ωm/thickness: 40 mm
	Radius	0.0094 m
	Number of conductors	10 longitudinal
	Buried at depth	0.628 m
Pipe	Series resistance	0.0002845 Ω/km
	Coating parameters	Uncoated
	Radius	0.61–0.512 m
	Number of conductors	1 hollow
	Buried at depth	20.628 m

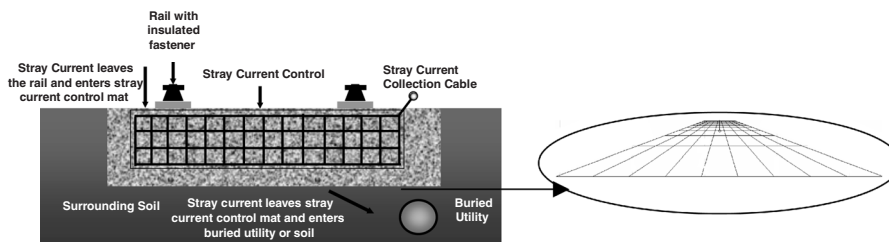


**Fig. 1** Cross-section of model used, showing path of stray current when rail is at a positive potential with respect to earth

the complexity of the stray current/trackbed mat placed underneath the rails. It is not necessary to simulate the inherent complexity in such a mat, and a simplification can be used as shown in Fig. 1.

The interconnected conductors shown in Fig. 1 form a flat metallic mat with the same series resistance as the real case and the same footprint/surface area. Tests using the software have shown that the number of longitudinal conductors in a real mat can be reduced significantly for modelling purposes, but a minimum of three are required. This simplification does not significantly affect the mutual resistance between model elements, errors of around 1% in the stray-current distribution being the result of this change. The benefit of simplifying the trackbed model lies in the lower number of conductors required by the CDEGS model and the corresponding decrease in runtime. As the conductors within a track bed are normally surrounded by concrete, the conductors are given a coating layer, which has the same resistivity and thickness as that of the concrete. This technique provides a method of modelling steel-reinforced concrete that can be placed in different soil environments. Simplification of the mat does, however, limit the ability of the model to examine the localised current distribution on the mat.

## 2.2 Soil models

The CDEGS software has a number of built-in soil models [3] applicable to different conditions. In this paper, simulations using uniform soils, two-layer horizontal soils and two-layer vertical-soil-resistivity environments are presented. Table 2 gives the specific details of the various models used.

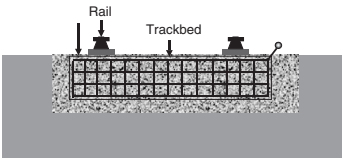
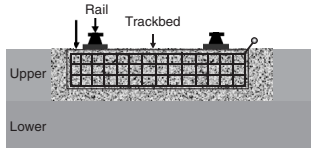
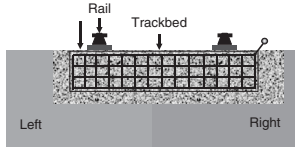
The uniform model allows all of the systems to be enclosed by the same soil resistivity (although the rails remain coated by a high-resistivity layer to permit simulation of the correct rail-to-earth resistance and the trackbed conductors are coated with a layer equivalent in thickness and resistivity to the cover provided by the trackbed concrete).

For the two-layer horizontal models, the rail and the track bed both lie in the top layer while the metallic pipe lies in the bottom layer. The track bed and rail are placed into the same environment, as they are in close proximity in real DC-traction systems.

For the two-layer vertical models, the rail, the metallic mat and the pipe all see a change in soil resistivity at a distance of 500 m, i.e. half of their length lies in high-resistivity soil while the other half lies in low-resistivity soil.

To assist in the understanding of the results presented later in the paper, Table 3 tabulates the resistance-to-earth values of the structures as determined by computer simulations for the soil environments employed in this study. The simulations took into consideration the fact that the buried metallic structures will mutually influence the resistance-to-earth values of the neighbouring components [10].

**Table 2: Models employed in simulations**

Uniform model			
Model A	10 Ωm		
Model B	100 Ωm		
Model C	1000 Ωm		
Two-layer horizontal model			
Model D	Top layer: 10 Ωm/bottom layer: 1000 Ωm		
Model E	Top layer: 1000 Ωm/bottom layer: 10 Ωm		
Model F	Top layer: 100 Ωm/bottom layer: 1000 Ωm		
Two-layer vertical model			
Model G	Left layer: 19 Ωm/right layer: 100 Ωm		
Model H	Left layer: 100 Ωm/right layer: 1000 Ωm		
Model I	Left layer: 10 Ωm/right layer: 1000 Ωm		

**Table 3: Series resistance and resistance to earth of DC-traction basic elements**

	Rail Resistance to earth (Ω km)	Series resistance (Ω km)	Trackbed Resistance to earth (Ω km)	Series resistance (Ω km)	Metallic pipe Resistance to earth (Ω km)	Series resistance (Ω km)
Uniform model						
Model A	319.9	0.040	0.046	0.080	0.016	0.0028
Model B	320.2	0.040	0.227	0.080	0.163	0.0028
Model C	322.8	0.040	1.985	0.080	1.578	0.0028
Two-layer horizontal model						
Model D	320.2	0.040	0.252	0.080	0.694	0.0028
Model E	321.7	0.040	0.847	0.080	0.017	0.0028
Model F	320.8	0.040	0.783	0.080	1.159	0.0028
Two-layer vertical model						
Model G	320.1	0.040	0.057	0.080	0.028	0.0028
Model H	321.3	0.040	0.377	0.080	0.286	0.0028
Model I	321.2	0.040	0.060	0.080	0.031	0.0028
Two-layer vertical model						
Model G	320.1	0.040	0.087	0.080	0.028	0.0028
Model H	321.3	0.040	0.411	0.080	0.286	0.0028
Model I	321.2	0.040	0.060	0.080	0.031	0.0028

When studying the Table of series resistances and resistances to earth of the metallic structure, it is clear that the resistance to earth in the uniform cases are proportional to soil resistivity for the metallic pipe and the track bed. For the rail, no significant change can be seen in the values of the resistance to earth, as the rail-to-earth insulation dominates this and not the soil resistivity.

For the two-layer horizontal model, the top layer of the model has a thickness of 15 m. The effect of the second layer, for example model D against model A or model E against model C, on the resistance to earth of the trackbed is clearly demonstrated. The metallic pipe, located in the lower layer, is also affected by the higher layer, as demonstrated by the results given when comparing models E and A or models D and C.

For the vertical models, the resistance to earth of the trackbed and the metallic pipe in the section of the low-resistivity soil is slightly increased compared with the

resistance to earth of the corresponding low-uniform-soil model. These are clearly demonstrated when comparing models G and A, H and B, I and A. Additionally, it can be shown that the resistance to earth of the trackbed and the metallic pipe in the section of the high-resistivity soil of the vertical model slightly reduces when compared with the corresponding high-resistivity uniform soil.

Of all the parameters detailed in this study, the soil resistivity is likely to introduce the greatest source of error into the modelling process. The CDEGS software has itself been shown to be accurate by many researchers across the world and has been extensively verified. The models used in this paper are simplifications of a real system but these simplifications were used after confirming that they did not cause an error in any expected current/voltage of more than 1% as previously detailed. The soil resistivity is, however, difficult to measure and will change as a function of the seasons/weather conditions. Dawalibi *et al.* state that

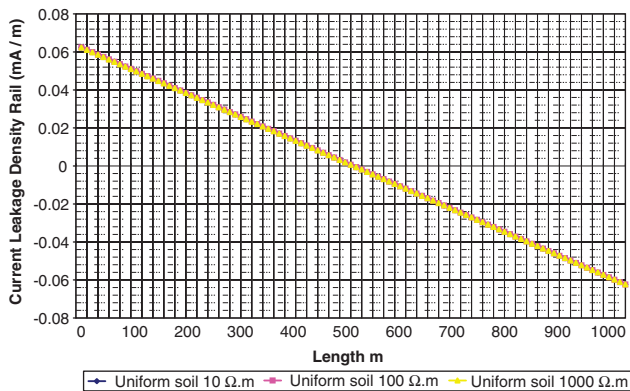
soil-resistivity measurements can be in error by as much as 50% when measurements are taken in proximity to metallic buried structures [10]. For a light-rail system being constructed in an urban environment, buried structures are likely to be present. Other researchers find that soil resistivities can change in a local environment by a factor of 20 according to the level of moisture present with a soil [11]. Soil near the earth boundary is likely to be significantly affected. It would therefore be prudent in any analysis to consider likely variations in soil resistivity over a year and the influence of buried objects on measurements before carrying out simulations.

### 3 Simulation results

#### 3.1 Uniform-soil models

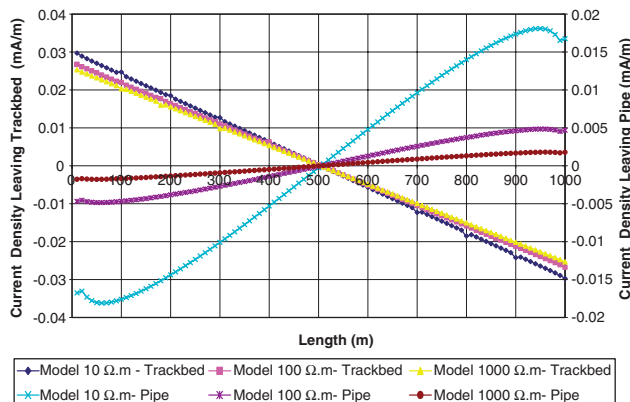
The leakage-current density of the rail is the same for all soil-resistivity models owing to the high resistance of the coating layer placed along the rail. Figure 2 illustrates the current-leakage-density profile for all three uniform-model cases. This profile arises from the running rail being at a positive potential with respect to earth at the location of the train and a negative potential with respect to earth at the substation.

Figure 3 illustrates the summated current-density profile from the trackbed's conductors and from metallic pipe into the soil for all three uniform-model cases. The main results from the uniform-soil models (A, B, C) are presented in Fig. 4 which gives the numerical values for the specific three soil-resistivity models described above. The measurements



**Fig. 2** Current-leakage density of rail

Current-density is expressed for these cases as amperes per metre of rail and not as amperes per unit rail surface area



**Fig. 3** Summated current-density profile from trackbed's conductors and from metallic pipe into the soil (uniform models)

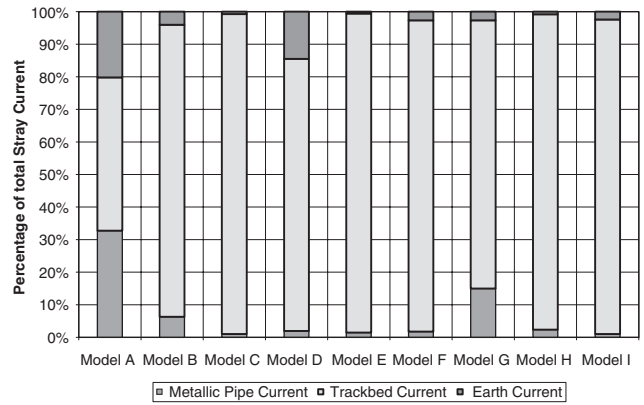


**Fig. 4** Change in proportion of stray current on the stated object for all models

Total stray current in all cases 1.57 mA = 100%

of the current flows are taken at the 500 m point where, for this symmetrical floating-rail system, no stray current is entering or leaving the rails.

The results are as expected, in that a higher soil resistivity ensures that a higher proportion of stray current is retained on the trackbed. This is due to the increasing resistance to earth of the trackbed compared with its series resistance which remains constant. The series path is made more attractive to stray current with increasing soil resistivity. In comparison, the stray current leaking onto the pipe shows a corresponding decrease, as does the current that remains within the earth layer.

For the uniform models, it is clear that the performance of the system can be expected to be constant over its length. This makes corrosion analysis, where stray-current densities are converted into gross charge over a period of system operation, simpler to achieve. A system can be analysed and the design of the rail insulation or stray-current-collection system can be altered if third party infrastructure is particularly vulnerable to damage.

#### 3.2 Two-layer horizontal-soil models

The three models simulated represent the cases where the soil resistivity increases with depth (model D), the case where the resistivity decreases with depth (model E) and the case where the two layers have soil resistivities that differ by a factor of 10 (model F) as opposed to the factor of 100 applied in the other two cases.

Figure 4 summarises the percentage of stray current found on each of the metallic structures and within the earth for the horizontal-layer simulations. Measurements of the current flows are again taken at the 500 m point where, for this symmetrical floating-rail system, no stray current is entering or leaving the rails.

The results of the horizontal soil models against uniform models can be compared with the aid of Fig. 4. By comparing the results of models D and A, F and B, E and C the effect of changing the bottom-layer soil resistivity is shown. Comparing models A and D, the bottom-layer resistivity increases from 10 Ωm to 1000 Ωm and the level of stray current retained on the trackbed is seen to increase. This relates to the increase in resistance to earth of the trackbed presented earlier in Table 3.

Comparing models B and F, a similar case is examined but the bottom-layer resistivity is only increased by a factor of 10 from 100 Ωm to 1000 Ωm. A similar result is found, but is reduced in severity.

When models C and E are compared, the performance of the trackbed stays reasonably constant even though the

bottom-layer resistivity has decreased significantly from  $1000\ \Omega\text{m}$  to  $10\ \Omega\text{m}$ , whereas the resistance to earth of the trackbed in the two layer soil model drops significantly, as should be the case [9–13].

Nonetheless the performance of the trackbed stays reasonably constant due to the high reflectivity factor at the boundary between top and bottom soil layers. When the upper-layer resistivity is large compared with that of the lower layer, as in model E, the reflection index is approximately 1 and current cannot penetrate into the lower layer [14]. Current can therefore not easily reach the pipe or the lower resistivity and is retained on the trackbed in a manner similar to that in the  $1000\ \Omega\text{m}$  uniform-soil model.

Figure 4 also illustrates the changes in the stray-current levels noted in the metallic pipe, which is always situated in the bottom layer of the horizontal model. The results correlate well with the changes in the level of current flowing in the trackbed. When models C and E are compared, no significant change in trackbed current can be observed and therefore no significant change is observed for the metallic pipe. When comparing A and D, more current is retained on the trackbed for the horizontal model as the bottom-layer resistivity increases. Less current is therefore observed on the metallic pipe.

### 3.3 Two-layer vertical-soil models

The analysis of the results for the vertical-soil models differs from that presented for the horizontal layers and uniform models, as a discontinuity in soil resistivity is introduced at some distance along the track. This has the effect of changing the current-leakage profiles from the trackbed and the pipe instantaneously. The rail-leakage profile is, again, not changed since its resistance to earth is primarily determined by the rail insulation that surrounds it.

Figure 5 shows the total amount of current leaking from a section of trackbed into the soil for each of the three models. The large discontinuities in the leakage current correspond to the change in soil resistivity. Where the soil is low resistivity (the left-hand 500 m of Fig. 5), and therefore the trackbed has a low resistance to earth, the level of leakage current is high. In the high-resistivity-soil section (the right-hand 500 m of Fig. 5), the level of leakage current reduces as the resistance to earth of the trackbed climbs. The difference on the current-density profiles in the cases where the soil models are uniform along the track length can clearly be seen by comparing Figs. 3 and 5. For the horizontal layered models the current-density profiles are also represented by straight line graphs with the same trend

as Fig. 3. (A comparison of the uniform and the horizontal-soil-model current distributions is shown in Fig. 4.) The discontinuities highlighted in Fig. 5 suggest that some portions of the system around the soil interfaces could be more at risk. Note that small discontinuities are present due to the use of interconnecting conductors placed on the mat at 100 m intervals, as shown in Fig. 1. These would be closer in a real system and the small discontinuities would not be present.

The leakage-current profile of the metallic pipe is also given in Fig. 5 and illustrates the profiles for the three cases. The graphs corresponding to the metallic pipe are effectively a mirror of the graphs corresponding to the trackbed. When the trackbed is allowing significant current to leak into the soil, the metallic pipe collects a portion of this. For the case where a small current is flowing from the mat, the pipe collects only small levels of current.

Table 4 tabulates the percentage of total stray current collected by the trackbed and the metallic pipe. In addition, the lengths of current-collection and current-leakage regions are also presented.

**Table 4: Proportion of total stray current on metallic structures: vertical models**

	Floating current	Collection region	Leakage region	Soil model
Total stray current	1.57 mA	502–1000 m	0–502 m	Model G
Metallic pipe	15.06%	0–341 m	341–1000 m	
Trackbed	82.91%	0–550 m	550–1000 m	
Earth current	2.66%			
Total stray current	1.57 mA	502–1000 m	0–502 m	Model H
Metallic pipe	2.38%	0–301 m	301–1000 m	
Trackbed	96.82%	0–502 m	502–1000 m	
Earth current	0.80%			
Total stray current	1.57 mA	502–1000 m	0–502 m	Model I
Metallic pipe	1.04%	0–291 m	291–1000 m	
Trackbed	96.57%	0–502 m	502–1000 m	
Earth current	2.4%			

Of particular significance in Table 4 is that the metallic pipe shows a significant variation in the region over which it is collecting or leaking stray current (Fig. 6). This is significant since, if current-leakage was to be concentrated over a small section of pipe in a real system, increased corrosion damage would occur on that section.

Note that the presence of a concentrated current-leakage region on the pipe depends not just on the presence of a vertical-soil model but also on the placement of the substation (i.e. in the high- or the low-resistivity layer). In the first case shown below, the substation is placed in the high-resistivity soil, while in the second case it is placed in the low-resistivity soil.

When the substation is in the high-resistivity soil, the metallic pipe collects current in the region 0–300 m. Where the substation is in the low-resistivity soil, the collection region extends from 0 to 700 m. Large levels of corrosive leakage-current density are therefore observed for the latter case.

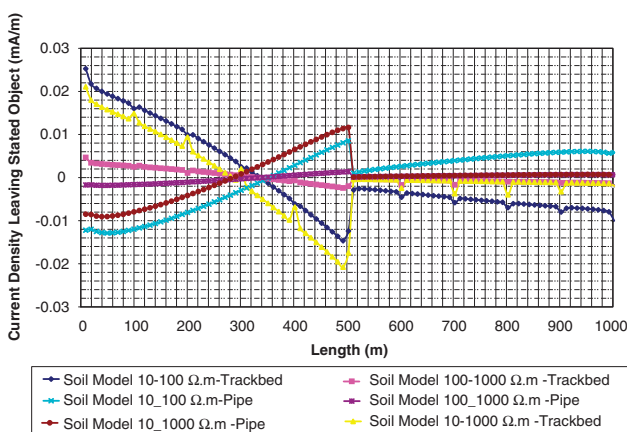


**Fig. 5** Summated current-density profile from trackbed's conductors and from metallic pipe into the soil (vertical models)

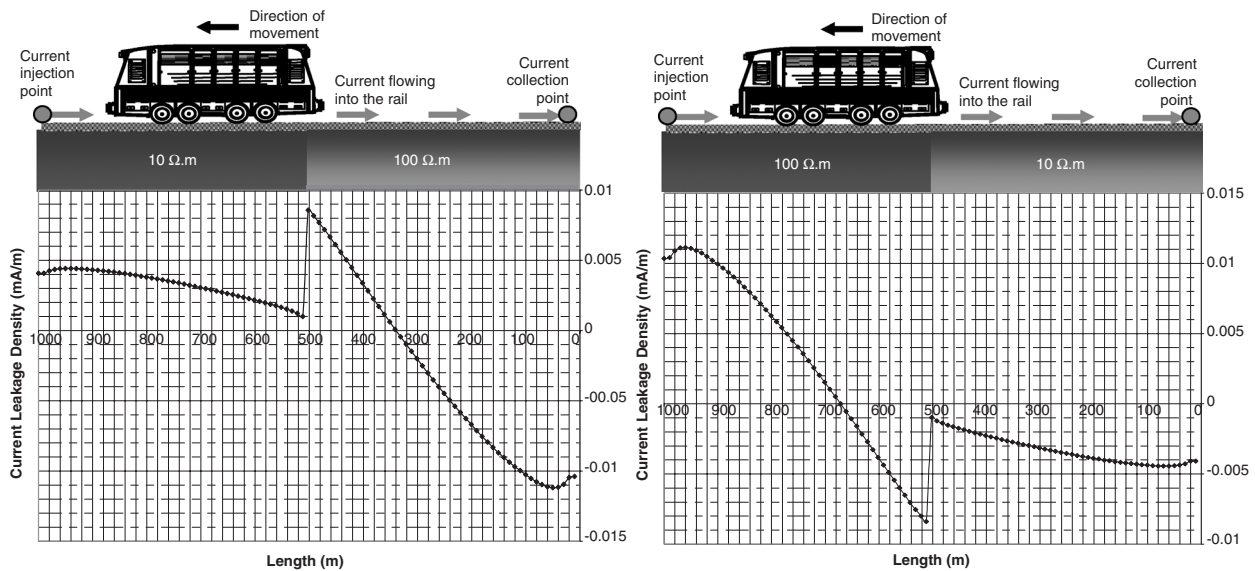


Fig. 6 Difference in pipe-leakage current-profile behaviour according to substation

#### 4 Dynamic modelling

True visualisation of the impact of the different soil models on the amount of corrosion seen on the transit system and the surrounding infrastructure is only possible using dynamic models. These dynamic models are essentially time-stepped static models in which the train position and velocity vary as a function of distance. In this Section, a simple dynamic model has been used in which a train is moved along a 1000m section of track while drawing a constant current (to represent running at constant velocity on a constant gradient).

By monitoring the total positive stray current (i.e. current leaking off a metallic structure) during each time step of the simulation, the total corrosive stray current can be obtained by its integration. This is defined as the gross leakage charge. Section 5 shows that, with the use of Faraday's law [8], which describes the amount of reduction that occurs in an electrolytic cell, the corrosion damage can then be obtained if required.

Figures 7 and 8 illustrate the corrosive leakage charge of the trackbed and the metallic pipe for uniform-soil models of 10, 100 and 1000 Ωm and additionally for the vertical-soil models of 10–1000 Ωm and 1000–10 Ωm.

First Fig. 7 illustrates the corrosive leakage charge of the base of the trackbed and the metallic pipe, respectively, for

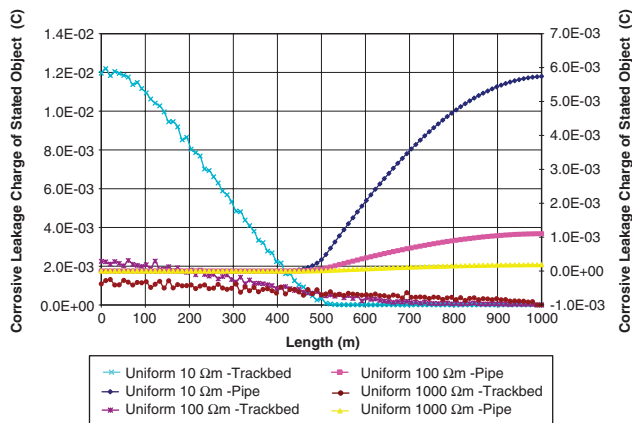


Fig. 7 Corrosive leakage charge of base of trackbed and metallic pipe

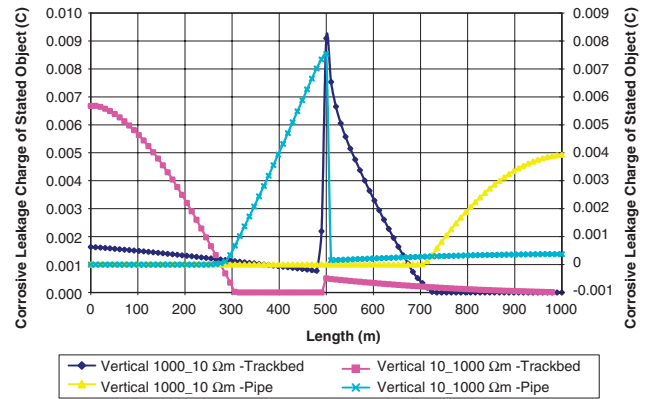


Fig. 8 Corrosive leakage charge of base of trackbed and pipe vertical-soil models

the three uniform models. Only the base of the trackbed is considered, since corrosion at the top of the trackbed is assumed to be proportional to the rail leakage current that is fairly invariant with soil resistivity.

It is obvious first that the graphs for each soil structure are mirrors of each other. This can be explained by considering the left-hand portion of Fig. 7 where stray current is positive and is leaking off the trackbed (therefore corroding it). This current must then leak onto the pipe, causing no corrosion damage. In the right-hand portion of Fig. 7, this trend is reversed. Figure 7 also illustrates the fact that, in homogenous systems, high soil resistivities mean that third-party buried structures are less vulnerable to corrosion damage while in low soil resistivities the converse is true.

Figure 8 illustrates the corrosive leakage charge of the trackbed and the metallic pipe, respectively, for the two vertical-soil models.

The results of the dynamical model for the vertical-soil models verify the conclusion stated previously, i.e. that a concentrated current-leakage region will exist on the pipe and trackbed when a vertical-soil model exists.

#### 5 Example modelling of a real system

The work detailed is intended to aid the accurate modelling of real transit systems. An example of the use of the

modelling in the analysis of a simple system is now presented.

The model consists of a 1 km track on which a train moves with a constant velocity and hence draws a constant current. The current used in this simulation is 1000 A. The results could be scaled linearly for other values of current. The example operational condition is that trains move along the section of track with a headway of 3 min. This will result in 20 trains running per hour. Assuming that services are running for 19 hours, i.e. from 5 am until midnight, the total number of trains that will run across the section under study would be 380. Therefore the total charge produced by the movement of 380 trains will be 380 times more than the charge produced by the operation of one train. The model must assess the cumulative impact of this stray current on the rails, the stray-current-collection system and any surrounding metallic infrastructure.

As an example of the approach taken to convert the values of current from the model to lifetime, ten interconnected 8 mm bars are used to form the stray-current mat placed under rail. When current leaks onto the mat (from the rail) and off the mat (into the soil), it is assumed that the current will be evenly distributed over the whole mat, but only on the half of the bar closest to the interface. This assumption is based on studies of an entire mat within the CDEGS software.

For 1 m of stray-current-control mat, the surface area vulnerable to corrosion is therefore  $0.5 \times \pi \times 10 \times 8 \text{ mm} \times 1000 \text{ mm} = 125\,664 \text{ mm}^2$  or  $0.126 \text{ m}^2$ . The current flowing onto/leaving the mat at a particular location can be converted to a current density using this area and the corrosion rate (for the areas where current is leaving the mat) can be determined using (3):

$$\text{Corrosion rate} = \frac{I_{\text{corr}}}{nF} \quad (3)$$

In (3),  $I_{\text{corr}}$  is the corrosion current density in amperes per square metre,  $F$  is Faraday's constant (96 490 C/mole), and  $n$  is the number of electrons transferred per molecule of a metal corroded. The corrosion rate is the number of corroded moles of metal per square metre per second, which converts to grams per square meter per day ( $\text{g/m}^2/\text{d}$ ), by multiplying by the atomic weight of the metal.

Figure 9 shows an example of the application of the model and this equation. This graph gives the metal loss that will be observed along the entire length of trackbed bars in one year, for a number of soil structures.

For oxygenated areas of the system, the depth of steel corrosion required to cause cracking of the concrete, and thus allow rapid penetration of chloride ions to the steel, is typically thought to be in the range of 150–200  $\mu\text{m}$ . Using this thickness to estimate the life of the system, Fig. 10

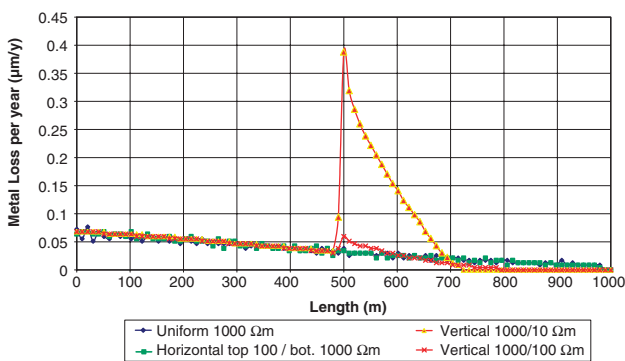


Fig. 9 Metal loss along the length of trackbed reinforcement

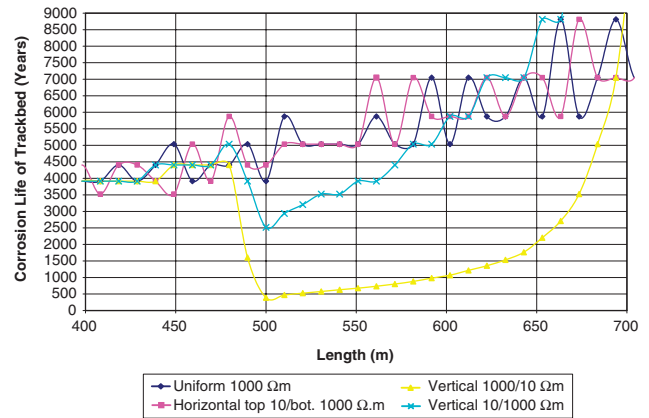


Fig. 10 Metal loss along the length of trackbed reinforcement after 120 years

illustrates the effect of the different soil structures on the corrosion-life calculation of a section of a trackbed based on the 150  $\mu\text{m}$  threshold.

In areas of the system with a lower lifetime, extra stray-current management in the form of upgraded rail insulation, larger trackbed conductors or a stray-current-control cable could be used to give a longer system lifetime.

## 6 Conclusions

The stray current produced by a floating-DC mass-transit system will adversely affect the transit system itself (rail) and any other metallic structure in the nearby vicinity. This paper demonstrates the influence of different soil models on the corrosion performance of the rail, trackbed and a metallic pipe.

For uniform soil layers it can be seen that, as the soil resistivity increases, the proportion of the stray current retained on the trackbed is increased while for the metallic pipe the proportion of the stray current is decreased as soil resistivity increases. Therefore it can be concluded that severe corrosion on pipelines predominates in sections where there is a low earth resistivity.

The performance of the trackbed when used as a stray-current-collection system (inadvertently or not) is highly dependent on the soil structure. As the soil resistivity increases with depth, the efficiency of the trackbed, i.e. the current retained on the trackbed, is significantly increased compared with the trackbed's efficiency for a uniform-soil-resistivity model. Furthermore, the corrosion risk on the metallic pipe significantly reduces as the soil resistivity increases with depth.

In the vertical-soil models, a nonuniform current-leakage density is observed. For the metallic pipe the most severe corrosion will occur in the layer where the soil resistivity is low. Additionally, the placement of the substation with respect to the earth layer (i.e. in the high- or the low-soil-resistivity region) will also help to determine the severity of corrosion.

Finally, the model can be used to optimise the level of stray-current protection required along the system length. To do this, accurate soil-resistivity information would be required and this would probably only be available for a new system.

## 7 References

- 1 Broomfield, J.P.: 'Corrosion of steel in concrete' (Spon, 1996), pp. 5–9
- 2 Sunde, E.D.: 'Earth conduction effects in transmission systems' (Dover Publications Inc., New York, 1968), pp. 184–196

- 3 'CDEGS Software': Safe Engineering Services & Technologies Ltd., Montreal, Quebec, Canada
- 4 Oslon, A.B., and Stankeeva, I.N.: 'Application of optical analogy to calculation of electric fields in multilayer media', *Electric Technology, USSR* 1979, No. 4
- 5 Cotton, I., Charalambous, C., Ernst, P., and Aylott, P.: 'Stray current control in DC mass transit systems', *IEEE Trans. Veh. Technol.*, 2005, **54**, (2), pp. 722–730
- 6 Yu, J.G.: 'The effects of earthing strategies on rail potential and stray currents in DC transit railways'. Proc. Int. Conf. Developments in Mass Transit Systems, April 1998
- 7 Case, S.: 'In DC traction stray current control – offer a stray a good Ohm?'. IEE Seminar Digest 212, 1999. pp. 1/1–1/6
- 8 Samuel, A.B.: 'Corrosion control' (Van Nostrand Reinhold, New York, 1993), pp. 4–8
- 9 Ma, J., Dawalibi, P., and Southey, R.D.: 'On the equivalence of uniform and two-layer soils to multilayer soils in the analysis of grounding systems', *IEE Proc.-Gener. Trans. Distrib.*, 1996, **143**, (1), pp. 49–55
- 10 Ma, J., and Dawalibi, F.P.: 'Study of influence of buried metallic structures on soil resistivity measurements', *IEEE Trans. Power Deliv.*, 1998, **13**, (2), pp. 356–365
- 11 He, J., Zeng, R., Gao, Y., Tu, Y., Sun, W., Zou, J., and Guan, Z.: 'Seasonal influences on safety of substation grounding system', *IEEE Trans. Power Deliv.*, 2003, **18**, (3), pp. 788–795
- 12 Nahman, J.M., and Djordjevic, V.B.: 'Resistance to ground of combined grid-multiple rods electrodes', *IEEE Trans. Power Deliv.*, 1996, **11**, (3), pp. 1337–1342
- 13 Dawalibi, F.P., Ma, J., and Southey, R.D.: 'Behaviour of grounding systems in multilayer soils: a parametric analysis', *IEEE Trans. Power Deliv.*, 1994, **9**, (1), pp. 334–342
- 14 Takahashi, T., and Kawase, T.: 'Calculation of earth resistance for a deep-driven rod in a multi-layer earth structure', *IEEE Trans. Power Deliv.*, 1991, **6**, (2), pp. 608–614